Segmental Alignment in the Aggregate Domains of Poly(9,9-dioctylfluorene) in Semidilute Solution

M. Habibur Rahman,[†] Chun-Yu Chen,[†] Shao-Ching Liao,[†] Hsin-Lung Chen,*[,†] Cheng-Si Tsao,[‡] Jean-Hong Chen,[§] Jing-Long Liao,[†] Viktor A. Ivanov,[||] and Show-An Chen[†]

Department of Chemical Engineering, National Tsing Hua University, Hsinchu 30013, Taiwan, Institute of Energy Research, Lungtun, Taoynan, Taiwan, Department of Polymer Materials, Kun Shan University, Yungkang City, Tainan Hsien 71003, Taiwan, and Physics Department, Moscow State University, Moscow 117234, Russia

Received May 8, 2007; Revised Manuscript Received June 26, 2007

ABSTRACT: The structure of poly(9,9-dioctylfluorene-2,7-diyl) (PF8) in deuterated toluene solutions at concentrations ranging from 0.60% to 7.0% (w/v) has been investigated by means of small-angle neutron scattering (SANS) and nuclear magnetic resonance (NMR) spectroscopy. PF8 chains exhibited aggregation above 1.0%, where the corresponding SANS profiles were characterized by the superposition of an aggregate component and a dynamic component associated with the transient network formed by interchain overlap. The ^{1}H NMR resonance lines for both the polymer as well as for the residual protons in the solvent showed large upfield shift at higher concentrations, indicating strong polymer−solvent interaction. At a higher concentration (4.5%) an additional resonance line was observed in the aromatic regions of both the ^{1}H and the ^{2}H spectra that has been attributed to a residual anisotropic chemical shift of the solvent molecules. The later phenomenon is suggestive of the existence of magnetically anisotropic aggregate domains of PF8 dispersed in an isotropic bulk.

1. Introduction

π-Conjugated polymers constitute a class of organic materials whose unique electrical and photonic semiconducting properties have led to a variety of optoelectronic applications ranging from light-emitting diodes[1] to photovoltaics.[2] These polymers are composed of rigid conjugated segments containing flexible short side chains to render nominal solubility in common organic solvents and hence make it easy to process the otherwise infusible and insoluble parent polymer. At the coarse-grained level, the segments of conjugated polymers can be represented as "hairy rods". These polymers are thus expected to develop liquid crystalline order, as rodlike molecules are known to form thermotropic as well as lyotropic liquid crystalline phases.[3]

Polyfluorenes (PFs) are a very attractive class of conjugated polymers[4−6] due to their great potential uses in blue-light emitting devices.[7,8] Poly[9,9-dioctylfluorene-2,7-diyl] (abbreviated as PF8, structure **1**) is a structural archetype of PFs having been extensively studied in the solid state as a model compound for the class.[9−23] PF8 is able to crystallize with the crystals melting at *ca*. 170 °C to a liquid crystalline phase up to the clearing temperature range of 270−280 °C.[24,25] The thermotropic LC phase of PF8 has been homogeneously aligned on treated surfaces and subsequently frozen into a nematic glass or slowly cooled to a crystalline film, both of which show strongly enhanced optical anisotropy in photoluminescence with a dichroic ratio of about 25.[26,27] Apart from the stable crystalline α-phase, the polymer exhibits a variety of metastable phases with characteristic photophysical properties depending on the processing condition. For example, in certain poor solvents and also upon the physical treatments of the solid polymer a mesomorphic phase that emits at a lower energy in photoluminescence (PL), commonly known as the β-phase, may develop. It is believed that these treatments induce twists between neighboring monomer units to facilitate a more planar backbone conformation and hence a more extended π-conjugation in this phase.[8−10,13−17,19]

Scheme 1. Structure of Poly[9,9-dioctylfluorene-2,7-diyl] (PF8, 1)

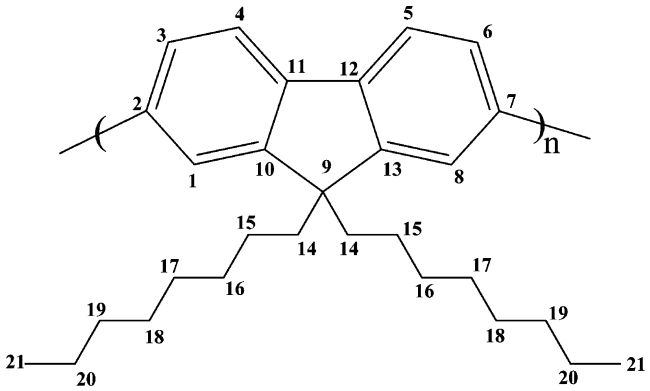

The application of π-conjugated polymers in optoelectronic devices requires thin films that can be suitably cast from appropriate solutions. Although the solution structure of the polymer greatly influences the morphology and the optoelectronic properties of the cast film,[9,28] only a few studies focusing on the dilute (≤1%) solution structure has been reported for PF8.[9,21] For instance, the conformational structure of PF8 in the solutions has been investigated by light scattering. The persistent length (l_{ps}) of the polymer deduced from the measured radius of gyration with the assumption of wormlike chain model indicates that the chain is semirigid with $l_{ps} \approx 8.5$ nm.[9] A recent study by small-angle neutron scattering (SANS) reveals that PF8 can be dissolved down to the molecular level in dilute (0.5−

* To whom correspondence should be addressed. E-mail: hslchen@mx.nthu.edu.tw.
[†] National Tsing Hua University.
[‡] Institute of Energy Research.
[§] Kun Shan University.
[||] Moscow State University.

10.1021/ma071036f CCC: $37.00
Published on Web 08/11/2007

1.0%) toluene solutions where they remain as stiff rods. By contrast, the dissolution only reaches the colloidal level giving rise to disklike aggregates in a poor solvent, methylcyclohexane (MCH).[21]

Herein we study the structure of PF8 in toluene solution over a broad concentration range (0.6%−7.0% (w/v)) using (NMR) spectroscopy as the major tool complemented with SANS results. We will demonstrate that the polymer shall undergo aggregation when the concentration exceeds 1.0%. The NMR study further reveals an unusual anisotropic diffusion mode of the solvent molecules suggesting that the segments in the aggregate domains are aligned, resembling a lyotropic liquid-crystalline (LC) state.

2. Experimental Section

Poly(9,9-dioctylfluorene-2,7-diyl) (PF8) end-capped with dimethylphenyl groups was obtained from American Dye Source, Inc., Quebec, Canada. Its molecular weight measured by GPC using THF as the eluting solvent and polystyrene as the standard was M_n = 49 800 and PDI = 2.0. Weighed amount of PF8 was first dissolved in 1 mL toluene-d_8 (99.6 atom% ^{2}H, Aldrich) by gently warming in a water bath at 50 °C and stirring overnight at room temperature (25 °C). 0.8 mL of this solution was transferred into the NMR tube (5 mm diameter) and capped with a rubber septum. It was subsequently degassed to remove dissolved oxygen by repeated freeze−thaw cycles, and the vacuum was released by dry nitrogen. The final concentration of the solutions before measurements were calculated from the height of the solution in the NMR tube calibrated to the volume. ^{1}H NMR spectra of the PF8 in toluene-d_8 solutions at temperatures ranging between −20 and +75 °C were measured at 499.84 MHz on a Varian UnityInova-500 NMR spectrometer at the Department of Chemistry of the National Tsing Hua University, Hsinchu, Taiwan. ^{2}H spectra were obtained by the same instrument at 76.73 MHz. A 1.0% solution and a 4.5% solution of PF8 in THF-d_8 (99.4 atom% ^{2}H, Aldrich) were similarly prepared and investigated by the NMR spectrometer.

SANS experiments were performed on the 30 m SANS instrument at the National Institute of Standard and Technology (NIST) Center for Neutron Research (NCNR).[29] The sample-to-detector distance was 30 m and the incident neutron wavelength λ was 8 Å with a wavelength dispersion, $\Delta\lambda/\lambda$ of 0.14.[30] This resulted in an effective q range of 0.0030 Å^{-1} < q < 0.40 Å^{-1}. The polymer solutions in deuterated toluene were encapsulated into quartz banjo cells having path lengths of 2 mm and were placed in the demountable titanium cell holder. The scattering intensity $I(q)$ was corrected for transmission, background, and parasitic scatterings and was normalized to an absolute intensity (scattering cross section per unit sample volume) as a function of the scattering vector q, where $q = (4\pi/\lambda)\sin(\theta/2)$, with λ and θ being the wavelength of the neutrons and the scattering angle, respectively.[31a] The incoherent background from the pure solvent was also measured, corrected by the volume fraction displaced by the dissolved PF8, and subtracted from the reduced scattering data.

3. Results and Discussions

3.1. SANS Study. Figure 1 shows the room-temperature SANS profiles in log−log plots of PF8/toluene solutions with concentrations ranging from 1.0% to 7.0%. The scattering intensity closely follows q^{-1} dependence in the high-q region (~ 0.03 Å^{-1} < q < ~ 0.11 Å^{-1}) irrespective of concentration, indicating the presence of rod entity under larger spatial resolution.[31b] The rods correspond to the hairy rod segments constituting the PF8 chain, as the molar mass per unit length (45.6 g mol^{-1} Å^{-1}) of the rods determined from the absolute intensity closely agrees with that calculated from the monomer unit of PF8 (=46.4 g mol^{-1} Å^{-1}).[9]

The scattering intensity tends to level off in the middle-q region (0.009−0.026 Å^{-1}) and shows an upturn at low q when the polymer concentration lies above 1.0%. The upturn of the low-q intensity attests that the hairy rod segments of PF8 undergo aggregation in toluene forming domains of aggregated chain segments that dominate the low-q intensity.

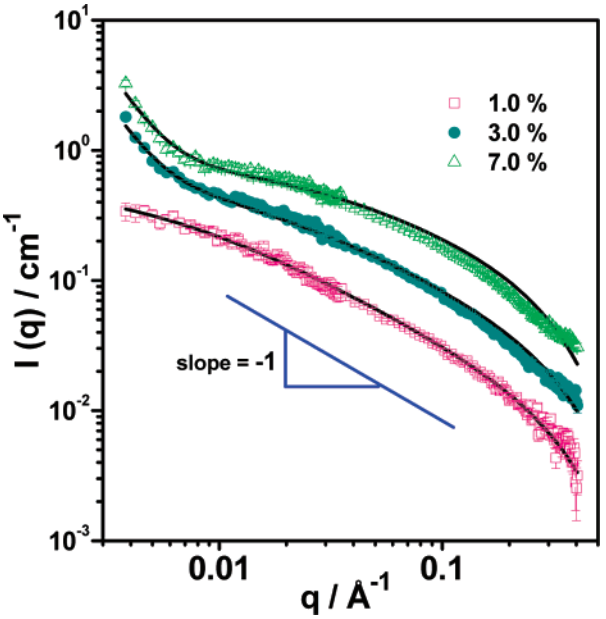

Figure 1. Room temperature (25 °C) SANS profiles of PF8/toluene-d_8 solutions at indicated concentrations (g of solute/100 mL solution). Solid curves are fits of the corresponding data to eq 5 (see text). The overlap concentration for the polymer used is ~0.8% (w/v) estimated from the square of the radius of gyration vs molar mass data of Grell et al.[9]

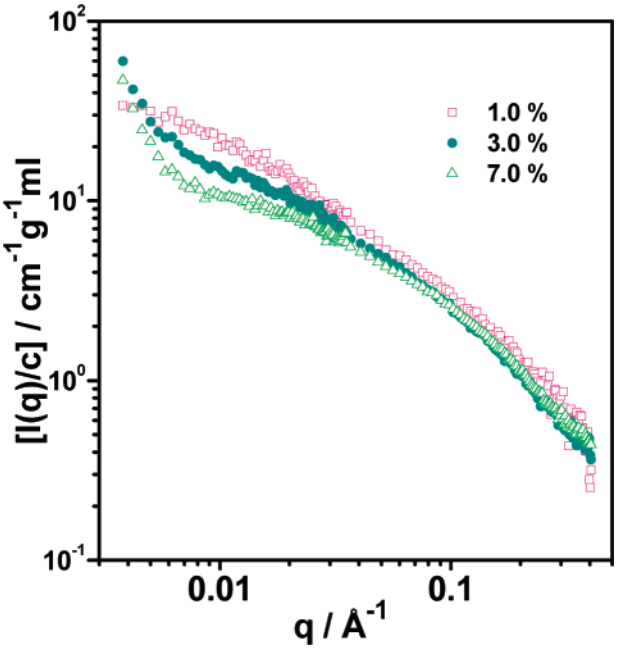

Figure 2. Concentration-normalized SANS profiles of PF8/toluene-d_8 solutions at indicated concentrations. The normalized intensity is independent of concentration in the high-q region whereas it decreases with increasing concentration in the middle-q region (0.009−0.026 Å^{-1}).

Further insight into the observed scattering patterns can be deduced from the concentration-normalized intensity profiles, $I(q)$/c, as displayed in Figure 2. It can be seen that the normalized intensity in the high-q region is independent of concentration, whereas at the middle-q it decreases with increasing concentration. This feature is prescribed by the transient network structure formed by the interchain overlap in

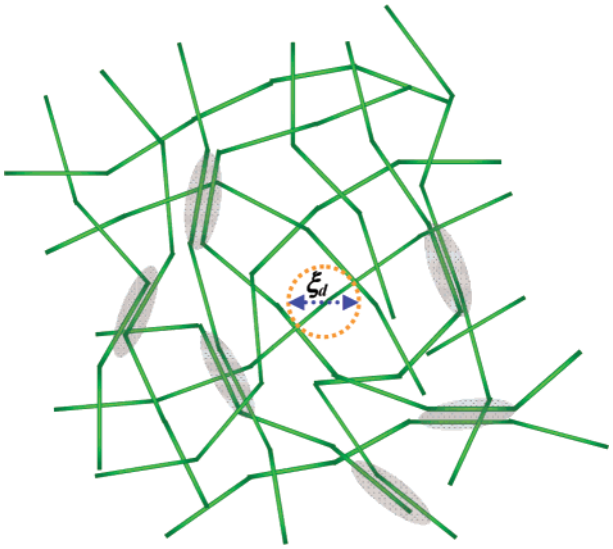

Figure 3. Schematic representation of the aggregate domains (shaded area) tying the PF8 chains to form a cluster. The overlap of the unassociated chains in the cluster as well as in the bulk of the semidilute solution generates a dynamic network with the characteristic mesh size of ξ_d.

the solution,[32] as illustrated schematically in Figure 3. In this case, the scattering intensity at $q > \xi_d^{-1}$ (ξ_d = mesh size of the dynamic network) is dominated by the form factor of the subchains (each enclosed by a blob as shown in Figure 3) between the dynamic overlap points. At $q < \xi_d^{-1}$ the solution may be described as a molten system of blobs with little fluctuations in density and thus the scattering intensity tends to level off.[32] For PF8, the subchains within the blobs are essentially rodlike as long as the mesh size is smaller than the Kuhn length. Therefore, the scattering intensity displays q^{-1} dependence at $q > \xi_d^{-1}$. The $I(q)/c$ associated with the transient network structure is proportional to the mesh volume ξ_d^3 at $q < \xi_d^{-1}$.[32] Normally the mesh size is smaller at higher polymer concentrations, such that $I(q)/c$ decreases with increasing concentration in the middle-q region.

Within the context of random phase approximation, the scattering intensity of a semidilute solution of ideal Gaussian chains is given by the Ornstein−Zernicke equation[33]

$$I(q) = \frac{I(0)}{(1 + q^2\xi_d^{\,2})} \tag{1}$$

where $I(0)$ is the zero-angle intensity proportional to $c\xi_d^3$. According to this equation, the scattering intensity displays an asymptotic power law of q^{-2}, which corresponds to the asymptotic behavior of the form factor of Gaussian chains. In the case where the subchains within the blobs are non-Gaussian, the scattering intensity is given by[33]

$$I(q) = \frac{I(0)}{[1 + (q\xi_d)^{1/\nu}]} \tag{2}$$

where ν is the scaling exponent of the dimension of subchains. For a swollen coil in good solvent $\nu = 0.6$.

The scattering intensity of the present system exhibits the asymptotic power law of q^{-1} followed by a steeper drop (at $q > 0.15$ Å^{-1}) due to the contribution of cross section of the rod subchains in the blobs. Therefore, the scattering intensity is given by

$$I(q) = \frac{I(0)}{[1 + \xi_d q \exp(q^2R^2/4)]} \tag{3}$$

in which R is the radius of the rod. This is a modified Ornstein−Zernicke equation modeling the scattering intensity arising from the transient networks with the mesh size being smaller than the Kuhn length.

In addition to the dynamic component due to the transient network, an additional component associated with the aggregation of a portion of the segments (cf. the shaded regions in Figure 3) contributes to the upturn of the low-q intensity for the 3.0 and 7.0% solutions. Here we adopt the well-known Debye−Bueche equation[34,35] to model this component,

$$I(q) = \frac{I_s(0)}{(1 + \xi_s^{\,2}q^2)^2} \tag{4}$$

where ξ_s is the correlation length which may characterize the average distance between the aggregate domains. The combination of eqs 3 and 4 yields the following two-component model for fitting the entire scattering curve:

$$I(q) = \frac{I_s(0)}{(1 + \xi_s^{\,2}q^2)^2} + \frac{I(0)}{[1 + \xi_d q \exp(q^2R^2/4)]} \tag{5}$$

The fitted results are shown by the solid curves in Figure 1 and the parameters obtained from the fits are shown in Table 1.

The dynamic mesh size is found to decrease with increasing overall concentration, which is consistent with the drop of $I(q)/c$ with increasing c observed in Figure 2. Figure 4 plots ξ_d as a function of overall concentration in log−log plot. The slope of the plot is *ca.* −0.89. For uniform dispersion of rod particles the mesh size scales as $c^{-1/2}$, and for flexible coils in Θ and good solvent the mesh size scales as $c^{-1}$and $c^{-3/4}$, respectively.[36] The exponent observed here is not consistent with that prescribed by any of the three cases. This can be attributed to the aggregation of the chains at the concentrations 3.0% and 7.0%, which yield network clusters. In these clusters the polymer chains are tied together by the aggregate domains (cf. Figure 3). The dynamic mesh size in the cluster network is expected to be smaller than that prescribed by the uniform dispersion of the polymer chains throughout the solution. It should be noted that the aggregate domains in the clusters formed at $c > 1.0\%$ should not be highly populated, as the dominance of the dynamic component in the SANS profiles indicates that most meshes in the system are "dynamic meshes". This is in clear distinction with the constrained networks formed by the prevalent aggregation of another conjugated polymer, DP6-PPV, in toluene.[37] The SANS profiles of these constrained networks have been found to exhibit well-defined power laws characterizing their fractal dimensions. The aggregate structure observed here is also different from the compact disklike aggregates formed by the same polymer in the even poorer solvent, MCH.[21]

3.2. NMR Study. Figure 5 shows the 500 MHz ^{1}H NMR spectra of 0.60% and 4.5% solutions of PF8 in toluene-d_8 at 25 °C. The spectra contain all the assigned[38] proton resonance lines of the polymer along with signals from the residual protons in the solvent. The resonance lines due to the polymer are broad in general; however, the spectrum of 0.60% solution is much better resolved than that of the 4.5% solution. Also, the ^{1}H resonance frequencies of PF8 in the former solution show close proximity with those in the literature in a dilute $CDCl_3$

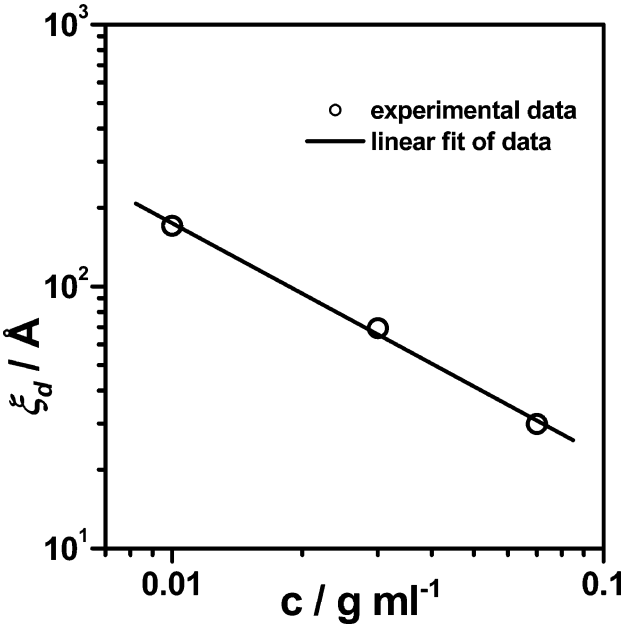

Figure 4. Log−log plot of dynamic mesh size as a function of overall polymer concentration.

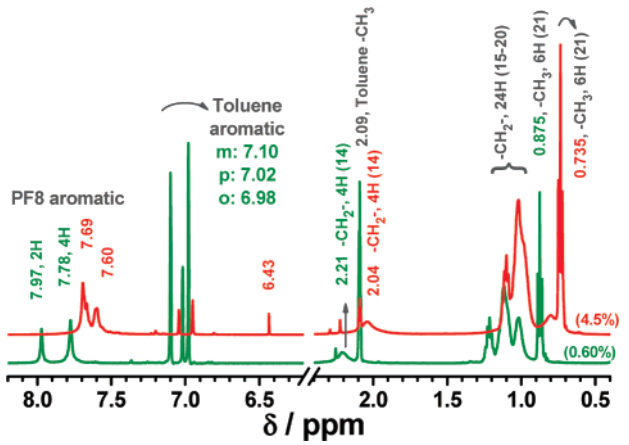

Figure 5. 500 MHz ^{1}H NMR spectra of 0.60% and 4.5% PF8 solutions in toluene-d_8 at 25 °C. The signal from the residual solvent protons (0.40 atom% H) centered at 2.09 ppm is used as the reference. Numbers in parentheses refer to Structure 1.

Table 1. Parameters Obtained from the Fit of the SANS Profiles to Eq 5

concn (%)	$I_s(0)$ (cm^{-1})	ξ_s (Å)	$I_d(0)$ (cm^{-1})	ξ_d (Å)	R (Å)
1.0			0.58 ± 0.01	170.1 ± 5.0	3.3 ± 0.2
3.0	28.9 ± 12.5	550.8 ± 87.2	0.68 ± 0.03	69.2 ± 4.5	3.3 ± 0.1
7.0	45.3 ± 22.1	514.7 ± 78.4	0.86 ± 0.03	29.8 ± 2.5	3.7 ± 0.3

solution.[38] All the resonance lines of the 4.5% solution shift to frequencies significantly lower than the corresponding lines of the 0.60% solution. Moreover, the spectra of the 4.5% solution contain an additional line in the aromatic region (6.43 ppm).

Figure 6 shows the NMR spectra of the 4.5% solution collected at temperatures between 5.0 and 75 °C. The resonance positions of the residual aromatic protons of the solvent in the solution[39] shift to frequencies (*meta*: 7.07 → 7.03 ppm)[40] much lower than the corresponding motionally narrowed resonance lines of the neat solvent as a function of temperature (7.11 → 7.07 ppm; inset of Figure 6). The additional absorption line in the aromatic region shifts gradually to higher frequencies (6.17 → 6.56 ppm) as the temperature is raised.

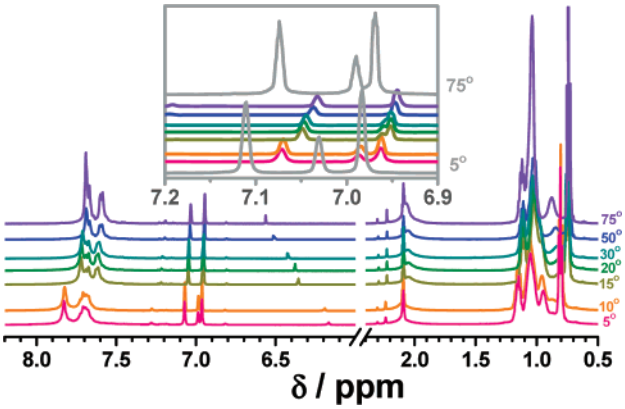

Figure 6. 500 MHz ^{1}H NMR spectra of a 4.5% PF8 solution in toluene-d_8 at indicated temperatures. The signal from the residual methyl protons in the solvent centered at 2.09 ppm was used as the reference. Inset: Expanded view of the residual aromatic proton resonances of the solvent in the solution at corresponding temperatures (in color). The same region in neat toluene-d_8 at indicated temperatures are shown for comparison (in gray).

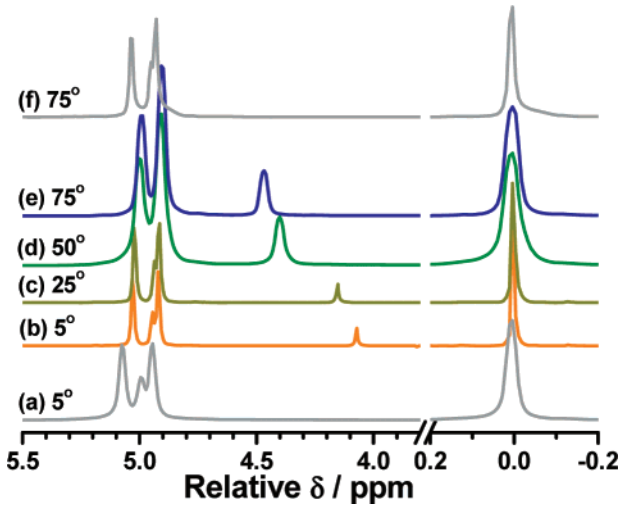

Figure 7. 76.73 MHz ^{2}H spectra: (a and f) Neat toluene-d_8, (b−e): 4.5% PF8 solution in toluene-d_8 at indicated temperatures. δ values refer to the resonance signal from methyl deuterons set at zero ppm.

Although the motionally narrowed line shape of the residual aromatic protons of neat toluene-d_8 is retained in the solution at lower temperatures, at higher temperatures the shape changes dramatically. The line due to the *para*-proton[40] gradually approaches toward that due to the *ortho*-protons at lower frequencies, first creating a shoulder and eventually merging with the latter at higher temperatures, while the additional peak shifts in the opposite sense (toward higher frequencies, see Figure 6).

76.73 MHz ^{2}H spectra of the same sample are shown in Figure 7. The extra line in the aromatic region is also prominent here confirming its association with the solvent. While the shape of the resonance lines of the aromatic region of pure toluene-d_8 persists at 5.0 and 25 °C, at higher temperatures the shape changes to a great extent: The lines due to the aromatic deuterons of the solvent shifts to lower frequencies with the *para*-deuteron resonance having a higher rate of the upfield shift, merges with the line due to the *ortho*-deuteron. On the other hand, the additional resonance line shifts to higher frequencies with increasing temperature. It is also noticed that the width of the ^{2}H resonance lines of the solution remarkably broadens at higher temperatures, contrary to what one should expect from

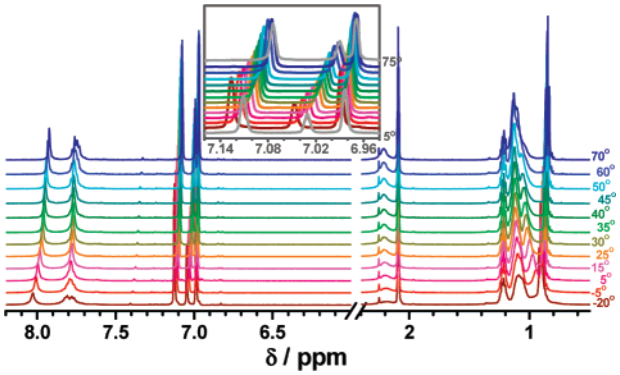

Figure 8. 500 MHz ^{1}H NMR spectra of a 0.60% PF8 solution in toluene-d_8 at indicated temperatures. Inset: Expanded view of the residual aromatic proton resonances of the solvent at corresponding temperatures (color coded). The same region in neat toluene-d_8 at indicated temperatures are shown for comparison (in gray).

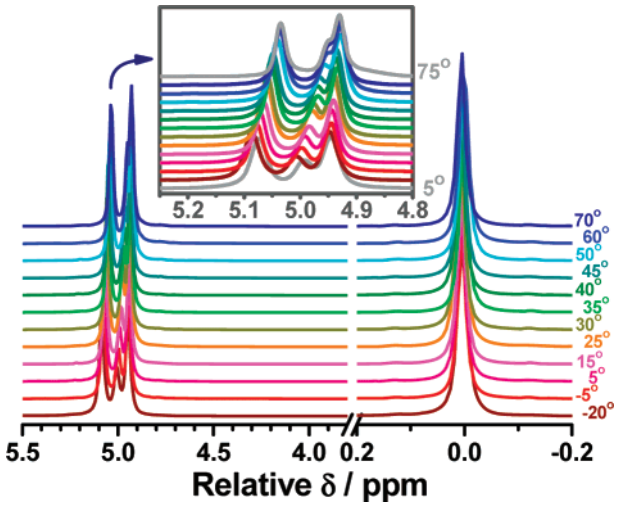

Figure 9. 76.73 MHz ^{2}H spectra of 0.60% PF8 solution in toluene-d_8 at indicated temperatures. δ values refer to the resonance signal from methyl deuterons set at zero ppm. Inset: Expanded view of the aromatic region at corresponding temperatures (color coded). The same region of neat toluene-d_8 at 5 and 75 °C are shown for comparison (in gray).

enhanced thermal Brownian diffusion of the solvent molecules (compare with spectra a and f of the solvent in Figure 7).

^{1}H and ^{2}H NMR spectra of the 0.60% PF8 in toluene-d_8 solution are displayed in Figure 8 and Figure 9, respectively. Both the spectra show regular shift in the motionally narrowed resonance lines of the aromatic region of the solvent with temperature. No additional resonance lines can be observed in the aromatic region of the spectra. The resonance lines in the ^{2}H spectra are not broadened to any significant extent either.

The presence of an extra resonance line in the 4.5% solution due to a solvent aromatic proton that persists up to 70 °C (highest studied temperature) along with its strong temperature dependency leads us to think of two domains for the reorientational Brownian diffusion of the solvent molecules in this solution: (a) an isotropic domain, where rotations of toluene molecule about its principal rotation axes[41] are motionally averaged giving rise to the resonance lines characteristic of the pure liquid, and (b) an anisotropic domain, where some of the rotational diffusion modes are only partially averaged, giving rise to a residual anisotropic chemical shift (RAS).[42] This is consistent with the formation of aggregate domains of PF8 segments of the lyotropic LC type dispersed in the isotropic solution matrix since the LC domains orient in the strong magnetic field of the NMR with their director parallel to the field direction[43] and the rotational diffusion of the solvent molecules local to the LC domains is known to be anisotiropic.[44] In the bulk of the solution, however, the environment for the Brownian diffusion of the solvent is isotropic. Existence of similar lyotropic aggregate domains (droplets) in equilibrium with the isotropic bulk phase at ambient temperatures has been speculated in a recent study in dilute toluene solutions of another hairy-rod conjugated polymer, poly(2,5-di-*n*-dodecyl-1,4-phenylene) by osmometry and transmission electron microscopy.[45] The observed extra resonance line can be presumed to be due to the RAS of the *para*-proton (deuteron) in toluene, as the line due to the *para*-proton suffers a larger rate of upfield shift with increasing temperature and eventually merges with the line for the *ortho* proton (cf. Figure 7 and inset of Figure 6). The reason why only the *para* proton gives rise to the RAS and not the other solvent protons lies in the complex dynamics of the solvent molecules[41] local to the aggregate domains, of which we do not have a complete understanding as yet. However, in order to minimize the extra magnetic energy ($E = -\chi B^2$, χ is the molar diamagnetic susceptibility) incurred from large induced currents in the aromatic ring in the magnetic field (B), toluene molecules would tend to orient with the plane of the molecule (along which χ is minimum) parallel to the field direction.[43] It turns out that the C_2 molecular axis (containing the plane of the aromatic ring and the *para* C−H bond) of toluene has a preference for orientation along the direction of the static magnetic field and as such, the shift anisotropy for the *para*-proton being not averaged completely, gives rise to the residual anisotropic shift. We can observe the two separate resonance lines for the *para*-proton because the rate of exchange of the solvent molecules between the two domains is rather slow on the NMR time scale. However, as the temperature rises, increasing rate of exchange of the solvent molecules between the two domains contributes to the gradual averaging of the two signals (they approach each-other) suggesting that the exchange rate is in fact comparable with the chemical shift difference between the two sites ($\tau^{-1} \approx |\delta_1 - \delta_2|$, intermediate exchange regime).[46] The unusual fattening of the solvent resonance signals much prominent at higher temperatures in the ^{2}H spectra of the 4.5% PF8 solution is due to the higher contribution of the exchange broadening[46] to the line width at higher temperatures. The protons (deuterons) in toluene other than the *para* one might also have produced RAS to small extents and contributed to the line broadening. The formation of aggregate domains is, however, not reflected in NMR study of the dilute solution (0.60%). These results nicely go with the SANS profiles of the solutions that have been characterized by the superposition of an aggregate component and a dynamic component in the 3.0% and the 7.0% solutions with the aggregate component being absent from the 1.0% solution.

Now the question remains as to the molecular mechanism for the formation of the aggregate domains. It is known that π-conjugated systems containing aromatic moiety are able to form aggregate domains through $\pi-\pi$ stacking in solution.[47] For efficient stacking, a planar conformation of the backbone has been presumed.[48] In such systems, an upfield shift in the ^{1}H NMR resonance lines from the aromatic protons with increasing concentration has been observed.[48,49] While such interactions may be the dominant mechanism for aggregation in aliphatic solvents, in aromatic solvents the solute−solute $\pi-\pi$ interaction should be unimportant due to the predominance of the solute−solvent $\pi-\pi$ interactions in the system. We have observed that the aromatic proton resonance lines of PF8 in 4.5% toluene-d_8 solution shifts upfield by a large extent (0.28

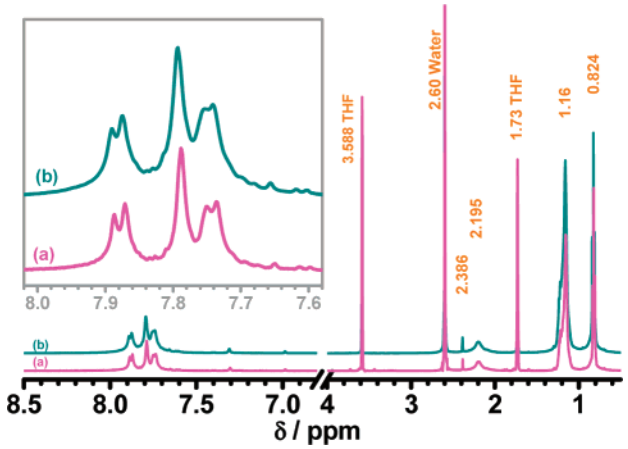

Figure 10. 500 MHz ^{1}H NMR spectra of 1.0% (a) and 4.5% (b) PF8−THF-d_8 solutions at 25 °C.

ppm) relative to those for a 0.60% solution (cf. Figure 1). However, the signals from the residual aromatic protons of the solvent molecules as well as those from the aliphatic protons in the dioctyl side chains of the polymer also display a similar shift, indicating a strong polymer−solvent interaction. It seems that the $\pi-\pi$ interactions among the PF8 backbone and the toluene molecules may be a plausible mechanism for the aggregate domain formation. The slow rate of exchange of the solvent molecules between the aggregate domains and the bulk may also indicate a solute−solvent complex formation.

To substantiate the idea of polymer−solvent complex formation in the aromatic solvent, we further extended the NMR study in a nonaromatic, deuterated solvent, tetrahydrofuran (THF-d_8). The ^{1}H NMR spectra of a 1% solution and a 4.5% solution of PF8 in THF-d_8 are very much similar in respect of the shapes and the positions of the resonance lines (cf. Figure 10), indicating the absence of any polymer−polymer (or polymer−solvent) interactions in the system. The backbone aromatic protons give rise to all the three resonance lines that can be predicted from the structure (Scheme 1). The doublet centered at δ 7.879 ppm, the singlet at δ 7.788 ppm, and the other doublet centered at δ 7.742 ppm (in the 1.0% solution) can be assigned to the equivalent protons positioned at 4 and 5, at 1 and 8, and at 3 and 6, respectively. These spectra are rather comparable to the spectra of the 0.60% PF8/toluene-d_8 solution in which the formation of aggregate domains is not prominent either in the ^{1}H NMR or in the SANS study. Since THF is an aliphatic solvent, a solute−solute $\pi-\pi$ complex formation was highly probable in it. However, we find no sign of such complex formation in the spectra. The absence of polymer−polymer interaction in the PF8−toluene-d_8 system at higher dilutions (0.50−1.0%) has also been suggested previously from concentration-dependent SANS study.[21] The steric hindrance from the pendant dioctyl groups might have prevented the polymer−polymer $\pi-\pi$ interactions from coming into play. Thus, in the semidilute PF8/toluene solutions, it is more likely that a polymer−solvent complex rather than the polymer−polymer one is formed through $\pi-\pi$ interaction.

Conclusions

The solutions of PF8 with toluene-d_8 in the concentration range 0.60−7.0% have been studied by NMR and SANS. We find that at concentrations exceeding 1.0% some of the chains form clusters within which there are domains of aggregated segments that tie up the chains into the clusters. The aggregate domains that persist in the solution up to the highest temperature of the study (70 °C) resemble lyotropic LC domains in that they become aligned in the static magnetic field of the NMR spectrometer imposing the rotational diffusion of the solvent molecules local to these aggregate domains to be anisotropic. The exchange of the solvent molecules between the LC domains and the isotropic bulk is slow on the NMR time scale, giving rise to two separate resonance absorptions for the solvent aromatic proton/deuteron in ^{1}H/^{2}H spectra. The strong concentration dependence of the resonance frequencies from the aromatic protons of both the polymer and the solvent suggests strong polymer−solvent $\pi-\pi$ interaction in the system.

Acknowledgment. This work was supported by the National Science Council (NSC) of Taiwan under Grant Nos. NSC 95-2752-E-007-006-PAE and NSC 94-2218-E-007-049. The supports of NIST, U.S. Department of Commerce, and the National Science Foundation, through Agreement No. DMR-9986442, in providing the neutron research facilities used in this work are gratefully acknowledged. Thanks are also due to Dr. Derek L. Ho at NIST for assistance in SANS experiment and helpful discussions. M.H.R. acknowledges the NSC for financial support in the form of a postdoctoral fellowship. He also acknowledges the University of Rajshahi, Bangladesh, for granting him study leave during the study.

References and Notes

(1) (a) Burroughes, J. H.; Bradley, D. D. C.; Brown, A. R.; Marks, R. N.; Mackay, K.; Friend, R. H.; Burns, P. L.; Holmes. A. B. *Nature (London)* **1990**, *347*, 539−541. (b) Gross, M.; Müller, D. C.; Nothofer, H.-G.; Scherf, U.; Neher, D.; Bräuchle, C.; Meerholz, K. *Nature (London)* **2000**, *405*, 661−665.
(2) Hoppe, H.; Sariciftci, N. S. *J. Mater. Res.* **2004**, *19*, 1924−1945.
(3) Donald, M.; Windle, A. H. *Liquid crystalline polymers*; Cambridge University Press: New York, 1992.
(4) Knaapila, M.; Stepanyan, R.; Lyons, B. P.; Torkkeli, M.; Monkman, A. P. *Adv. Funct. Mater.* **2006**, *16*, 599−609.
(5) Hoeben, F. J. M.; Jonkheijm, P.; Meijer, E. W.; Schenning, A. P. H. J. *Chem. Rev.* **2005**, *105*, 1491−1546.
(6) Neher, D. *Macromol. Rapid Commun.* **2001**, *22*, 1365−1385.
(7) Akcelrud, L. *Prog. Polym. Sci.* **2003**, *28*, 875−962.
(8) Cadby, J.; Lane, P. A.; Mellor, H.; Martin, S. J.; Grell, M.; Giebeler, C.; Bradley, D. D. C. *Phys. Rev. B* **2000**, *62*, 15604−15609.
(9) Grell, M.; Bradley, D. D. C.; Long, X.; Chamberlain, T.; Inbasekaran, M.; Woo, E. P.; Soliman, M. *Acta Polym.* **1998**, *79*, 439−444.
(10) Grell, M.; Bradley, D. D. C.; Ungar, G.; Hill, J.; Whitehead, K. S. *Macromolecules* **1999**, *32*, 5810−5817.
(11) Ariu, M.; Lidzey, D. G.; Bradley, D. D. C. *Synth. Met.* **2000**, *111*−*112*, 607−610.
(12) Kawana, S.; Durrell, M.; Lu, J.; MacDonald, J. E.; Grell, M.; Bradley, D. D. C.; Jukes, P. C.; Jones, R. A. L.; Bennett, S. L. *Polymer* **2002**, *43*, 1907−1913.
(13) Winokur, M. J.; Slinker, J.; Huber, D. L. *Phys. Rev. B* **2003**, *67*, 184106 (1−11).
(14) Misaki, M.; Ueda, Y.; Nagamatsu, S.; Yoshida, Y.; Tanigaki, N.; Yase, K. *Macromolecules* **2004**, *37*, 6926−6931.
(15) Rothe, C.; King, S. M.; Dias, F.; Monkman, A. P. *Phys. Rev. B* **2004**, *70*, 195213 (1−10).
(16) Chen, S. H.; Chou, H. L.; Su, A. C.; Chen, S. A. *Macromolecules* **2004**, *37*, 6833−6838.
(17) Chen, S. H.; Su, A. C.; Chen, S. A. *J. Phys. Chem. B* **2005**, *109*, 10067−10072.
(18) Chen, S. H.; Su, A. C.; Su, C. H.; Chen, S. A. *Macromolecules* **2005**, *38*, 379−385.
(19) Chunwaschirasiri, W.; Tanto, B.; Huber, D. L.; Winokur, M. J. *Phys. Rev. Lett.* **2005**, *94*, 107402 (1−4).
(20) Arif, M.; Volz, C.; Guha, S. *Phys. Rev. Lett.* **2006**, *96*, 025503 (1−4).
(21) Knaapila, M.; Garamus, V. M.; Dias, F. B.; Almásy, L.; Galbrecht, F.; Charas, A.; Morgado, J.; Burrows, H. D.; Scherf, U.; Monkman, A. P. *Macromolecules* **2006**, *39*, 6505−6512.
(22) Campoy-Quiles, M.; Sims, M.; Etchegoin, P. G.; Bradley, D. D. C. *Macromolecules* **2006**, *39*, 7673−7680.
(23) Chen, S.-H.; Su, A.-C.; Chen, S.-A. *Macromolecules* **2006**, *39*, 9143−9149.

(24) Bradley, D. D. C.; Grell, M.; Grice, A.; Tajbakhsh, A. R.; O'Brien, D. F.; Bleyer, A. *Opt. Mater.* **1998**, *9*, 1−11.
(25) Grell, M.; Bradley, D. D. C.; Inbasekaran, M.; Woo, E. P. *Adv. Mater.* **1997**, *9*, 798−802.
(26) Misaki, M.; Ueda, Y.; Nagamatsu, S.; Yoshida, Y.; Tanigaki, N.; Yase, K. *Macromolecules* **2004**, *37*, 6926−6931.
(27) Redecker, M.; Bradley, D. D. C.; Inbasekaran, M.; Woo, E. P. *Appl. Phys. Lett.* **1999**, *74*, 1400−1402.
(28) (a) Banach, M. J.; Friend, R. H.; Sirringhaus, H. *Macromolecules* **2004**, *37*, 6079−6085. (b) Nguyen, T.-Q.; Doan, V.; Schwartz, B. J. *J. Chem. Phys.* **1999**, *110*, 4068−4078.
(29) Glinka, J.; Barker, J. G.; Hammouda, B.; Krueger, S.; Moyer, J. J.; Orts, W. J. *J. Appl. Crystallogr.* **1998**, *31*, 430−445.
(30) Cold Neutron Research Facility at the National Institute of Standards and Technology, NG3 and NG7 30-Meter SANS Instruments Data Acquisition Manual, 1999.
(31) Higgins, J. S; Benoit, H. C. *Polymers and Neutron Scattering*; Claredon Press: Oxford, U.K., and New York, 1994: (a) p 10; (b) pp 165−169.
(32) de Gennes, P. G. *Scaling concepts in polymer physics*; Cornell University Press: Ithaca, NY, 1979.
(33) Rubinstein, M.; Colby, R. H. *Polymer Physics*; Oxford University Press: Oxford, U.K., and New York, 2003; p 189.
(34) Debye, P.; Bueche, A. M. *J. Appl. Phys.* **1949**, *20*, 518−525.
(35) Debye, P.; Anderson, H. R.; Brumberger, H. *J. Appl. Phys.* **1957**, *28*, 679−683.
(36) Strobl, G. *The Physics of Polymers*, 3rd ed.; Springer-Verlag: Berlin, 2007; Chapter 3.
(37) Li, Y.-C.; Chen, K.-B.; Chen, H.-L.; Hsu, C.-S.; Tsao, C.-S.; Chen, J.-H.; Chen, S.-A. *Langmuir* **2006**, *22*, 11009−11015.
(38) Ranger, M.; Rondeau, D.; Leclerc, M. *Macromolecules* **1997**, *30*, 7686−7691.
(39) CIL NMR Solvent Data Chart, Cambridge Isotope Laboratories, Inc., Web: www.isotope.com.
(40) Williamson, M. P.; Kostelnik, R. J.; Castellano, S. M. *J. Chem. Phys.* **1968**, *49*, 2218−2224.
(41) Sturz, L.; Dölle, A. *J. Phys. Chem.* **2001**, *105*, 5055−5060.
(42) Buckingham, D.; Burnel, E. E. *J. Am. Chem. Soc.* **1967**, *89*, 3341.
(43) (a) Christianen, P. C. M.; Shklyarevskiy, I. O.; Boamfa, M. I.; Maan, J. C. *Physica B* **2004**, *346−347*, 255−261. (b) de Gennes, P. G.; Prost, J. *Physics of Liquid Crystals*, Clarendon Press: Oxford, U.K., 1993.
(44) (a) Saupe, A.; Englert. G. *Phys. Rev. Lett.* **1963**, *11*, 462−464. (b) Snyder, L. C. *J. Chem. Phys.* **1965**, *43*, 4041−4050. (c) Panar, M.; Phillips, W. D. *J. Am. Chem. Soc.* **1968**, *90*, 3880−3382. (d) Diehl, P.; Khetrapal, L. C. In *NMR Basic Principles and Progress*; Diehl, P.; Fluck, E.; Kosfeld, R., (eds.); Springer-Verlag: New York, 1968; Volume 1.
(45) Harre, K.; Wegner, G. *Polymer* **2006**, *47*, 7312−7317.
(46) (a) Freeman, R. *A Handbook of Nuclear Magnetic Resonance*, 2nd ed.; Addison Wesley Longman Limited: Harlow, England, 1997; pp 31−35. (b) Sanders, J. K. M.; Hunter, B. K. *Modern NMR Spectroscopy: A Guide for Chemists*, 2nd ed.; Oxford University Press: Oxford, U.K., and New York, 1993; Chapter 7.
(47) Shetty, A. S.; Zhang, J.; Moore, J. S. *J. Am. Chem. Soc.* **1996**, *118*, 1019−1027.
(48) Blondin, P.; Bouchard, J.; Beaupré, S.; Belletête, M.; Durocher, G.; Leclerc, M. *Macromolecules* **2000**, *33*, 5874−5879.
(49) Niazimbetova, Z. I.; Christian, H. Y.; Bhandari, Y. J.; Beyer, F. L.; Galvin, M. E. *J. Phys. Chem. B* **2004**, *108*, 8673−8681.

MA071036F